Mechanically Durable Carbon Nanotube–Composite Hierarchical Structures with Superhydrophobicity, Self-Cleaning, and Low-Drag

Yong Chae Jung and Bharat Bhushan*

Nanoprobe Laboratory for Bio- & Nanotechnology and Biomimetics (NLB), The Ohio State University, 201 West 19th Avenue, Columbus, Ohio 43210-1142

ARTICLE

ABSTRACT Superhydrophobic surfaces with high contact angle and low contact angle hysteresis exhibit a self-cleaning effect and low drag for fluid flow. The lotus (*Nelumbo nucifera*) leaf is one of the examples found in nature for superhydrophobic surfaces. For the development of superhydrophobic surfaces, which is important for various applications such as glass windows, solar panels, and microchannels, materials and fabrication methods need to be explored to provide mechanically durable surfaces. It is necessary to perform durability studies on these surfaces. Carbon nanotube (CNT), composite structures which would lead to superhydrophobicity, self-cleaning, and low-drag, were prepared using a spray method. As a benchmark, structured surfaces with lotus wax were also prepared to compare with the durability of CNT composite structures. To compare the durability of the various fabricated surfaces, waterfall/jet tests were conducted to determine the loss of superhydrophobicity by changing the flow time and pressure conditions. Wear and friction studies were also performed using an atomic force microscope (AFM) and a ball-on-flat tribometer. The changes in the morphology of the structured surfaces were examined by AFM and optical imaging. We find that superhydrophobic CNT composite structures showed good mechanical durability, superior to the structured surfaces with lotus wax, and may be suitable for real world applications.

KEYWORDS: durability · CNT · lotus · hierarchical structure · superhydrophobicity

Superhydrophobic and self-cleaning surfaces with a high static contact angle above 150° and low contact angle hysteresis (the difference between the advancing and receding contact angles) play an important role in technical applications including self-cleaning window glasses, paints, textiles, solar panels, and applications requiring antifouling and reduction of drag for fluid flow in microchannels and for energy conservation.[1–4]

Lotus (*Nelumbo nucifera*) leaves have been the inspiration for the development of several commercially available superhydrophobic, self-cleaning, and low-drag products.[5–7] The lotus plant surface, which has an intrinsic hierarchical structure built by convex cell papillae and randomly oriented hydrophobic wax tubules, exhibits a very low water contact angle hysteresis, on the order of 3°, which is responsible for water droplets rolling off (with some slip) of the surface and taking contaminants with them, providing the self-cleaning ability known as the lotus effect. The crucial points required for the development of self-cleaning materials are superhydrophobicity and low contact angle hysteresis. Hierarchical structure provides air pocket formation, leading to the lowest contact area of applied water droplet (Figure 1), resulting in the reduction of contact angle hysteresis, tilt angle, and adhesive force.[2–4,8,9]

On the basis of the understanding of nature, a number of artificial hydrophobic surfaces have been fabricated with hierarchical structures using electrodeposition, colloidal particles, photolithography, soft lithography, plasma treatment, self-assembly, and imprinting.[4,10–18] Since many applications operate in long-term exposure to various liquids and are exposed to rough operating conditions, hydrophobic surfaces should have mechanical strength and chemical stability. Therefore, it is necessary to perform durability studies on these surfaces in order to identify fabrication techniques and materials that can best be used in real world applications.

It is of interest to create structured surfaces using carbon nanotubes (CNTs) for various applications, including mimicking the lotus effect and gecko feet due to their mechanical strength combined with their low density.[19–24] Various studies have also demonstrated that the use of CNTs in composites with various materials can considerably improve the mechanical properties and tribology.[25–30] Molding is a low cost and reliable way of microstructure replication and can provide a precision on the order of 10 nm,[31,32] and the spray method is

*Address correspondence to Bhushan.2@osu.edu.

Received for review October 28, 2009 and accepted November 19, 2009.

Published online November 30, 2009.
10.1021/nn901509r

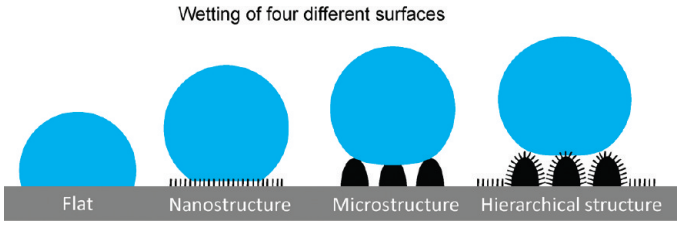

Figure 1. Schematic and wetting of the four different surfaces fabricated. The largest contact area between the droplet and the surface is given in flat and microstructured surfaces, but is reduced in nanostructured surfaces and is minimized in hierarchical structured surfaces.

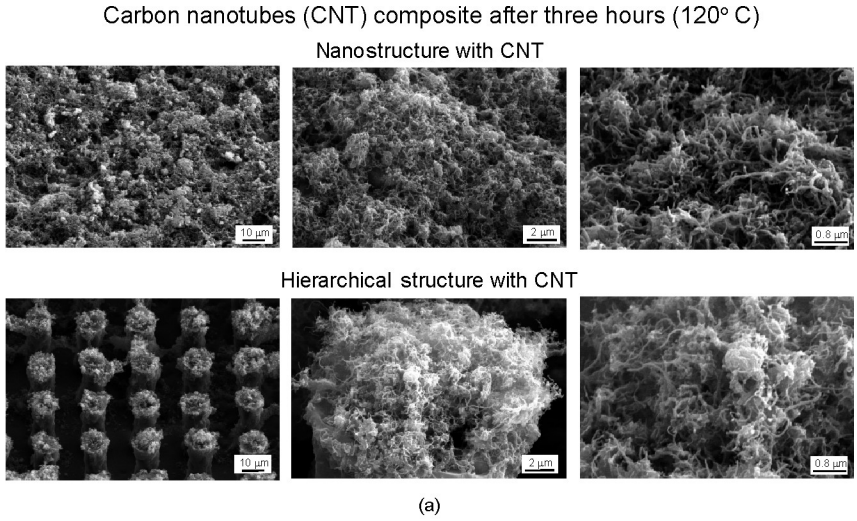

Figure 2. SEM micrographs taken at 45° tilt angle, show three magnifications of (a) nano- and hierarchical structures fabricated with CNTs after 3 h at 120 °C, and (b) nano-, micro-, and hierarchical structures fabricated with mass 0.8 μg/mm² of lotus wax after storage for 7 d at 50 °C with ethanol vapor.[17]

an easy and convenient method to deposit CNT composites to the substrate.[33,34] Nanostructuring of CNTs using the spray method over a molded microstructure can provide flexibility in the fabrication of a variety of hierarchical structures. This flexible technique has been used in this paper to produce nano- and hierarchical structures with CNTs.

A suitable characterization technique for mechanical durability is needed for technical applications that can resolve the small changes during sliding. Atomic force microscopy (AFM) and ball-on-flat tribometer are well-suited for this purpose as these have the ability to measure tribological properties. An AFM, which is a typical example of a scanning probe technique, detects minute forces between the sample surface and the scanning tip attached to a cantilever.[1,35,36] An AFM tip sliding on the sample surface simulates a single asperity contact under lightly loaded conditions typically encountered during device operation. For an application with high loads, comprehensive investigations of friction and wear behavior of structured surfaces can be conducted using the conventional ball-on-flat tribometer.[37−39] In this test method, a stationary ball applies a constant normal load while sliding on the sample surface.

In our recent studies, artificial structured surfaces with superhydrophobicity and self-cleaning have been produced using tubule forming waxes isolated from lotus leaves.[4,17] In the present study, to improve mechanical durability for superhydrophobicity and self-cleaning, for the first time, CNT composite structures were created using a spray method. As a benchmark, we have used surfaces with lotus wax. To investigate the durability of the fabricated surfaces, waterfall/jet tests were conducted to determine the loss of superhydrophobicity, and wear and friction studies were also performed using AFM and ball-on-flat tribometer.

Figure 2 shows the scanning electron microscope (SEM) micrographs of nano-, micro-, and hierarchical structures fabricated with CNTs and lotus wax. SEM micrographs show an overview (left column), a detail in higher magnification (middle column), and a large magnification of the nanostructures with CNTs and lotus wax and the created flat lotus wax layer (right col-

umn). All surfaces show a homogeneous distribution of CNTs and lotus wax on the specimen. Figure 2a shows that the CNTs were well dispersed and embedded on flat and microstructured surfaces for the desired nanostructure. The CNT diameter varied between 10 and 30 nm, and an aspect ratio varied between 160 and 200. The recrystallized lotus wax shows tubular hollow structures with random orientation on the surfaces as shown in Figure 2b. Their shapes and sizes show only a few variations. The tubular diameter varied between 100 and 150 nm, and their length varied between 1500 and 2000 nm.

RESULTS AND DISCUSSION

Wettability of Various Surfaces. To study the effect of CNT composite structures for superhydrophobicity, the static contact angle and contact angle hysteresis were measured on nano- and hierarchical structures with CNTs. For static contact angle and contact angle hysteresis, droplets of about 5 μL in volume (with the diameter of a spherical droplet about 2.1 mm) were gently deposited on the surface using a microsyringe. For contact angle hysteresis, the advancing and receding contact angles were measured at the front and back of the droplet moving along the tilted surface, respectively. Figure 3a shows that superhydrophobicity with a static contact angle of 166° and a contact angle hysteresis of 4° was found in the nanostructured surface with CNTs. After introducing CNT nanostructure on top of the micropatterned Si replica, the higher static contact angle of 170° and lower contact angle hysteresis of 2° were found for the hierarchical structures with CNTs. Both nano- and hierarchical structures created with CNTs showed superhydrophobic and self-cleaning surface, which has a static contact angle of more than 150° and contact angle hysteresis of less than 10°.

Figure 3b shows that for the hierarchical structure with lotus wax, the highest static contact angles of 173° and lowest contact angle hysteresis of 1° were found. The recrystallized wax tubules are very similar to those of the original lotus leaf, but are 0.5−1 μm longer, the static contact angle is higher, and the contact angle hysteresis is lower than reported for the original lotus leaf (static contact angle of 164° and contact angle hysteresis of 3°).[17] Superhydrophobicity with a static contact angle of 167° and a contact angle hysteresis of 5° was also found in the nanostructured surface with lotus wax. The microstructured surface with the lotus wax layer has a static contact angle of 160°, but shows a much higher contact angle hysteresis of 29° than found in hierarchical structures. Melting of the lotus wax led to a flat surface with a flat wax film and a much lower static contact angle of 119° and higher contact angle hysteresis of 71°. The data of a flat lotus wax film on a flat replica show that the lotus wax by itself is hydrophobic.

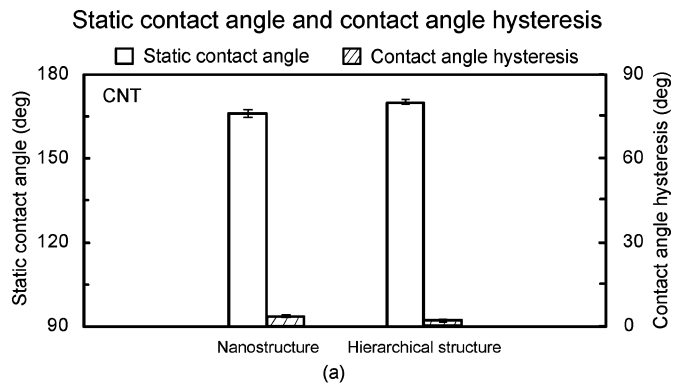

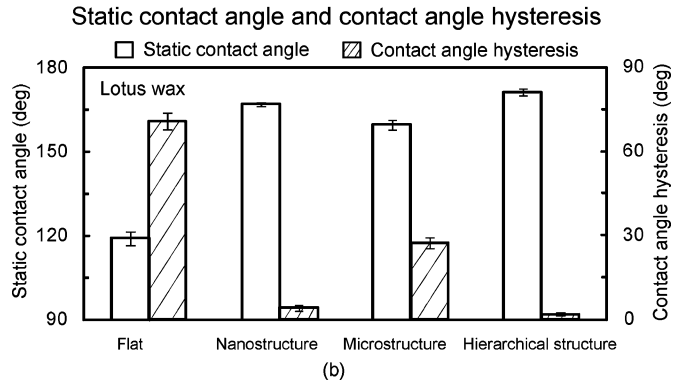

Figure 3. Bar chart showing the measured static contact angle and contact angle hysteresis on (a) nano- and hierarchical structures fabricated with CNTs after 3 h at 120 °C and (b) various structures fabricated with 0.8 μg/mm^2 of lotus wax after storage for 7 d at 50 °C with ethanol vapor.[17] The error bar represents ±1 standard deviation.

Durability of Various Surfaces in Waterfall/Jet Tests. To investigate the durability of the created surfaces in long-term exposure to water, and how different kinetic energies of the water hitting the surface affect wetting properties, waterfall/jet tests were conducted on the surfaces created with CNTs and lotus wax, First, the nano- and hierarchical structures with CNTs were continuously exposed to water pressure of 10 kPa for 24 h. Figure 4a (left side) shows static contact angle and contact angle hysteresis as a function of exposure time. In the case of nano- and hierarchical structures with CNTs, it was observed that the static contact angles decreased slightly but remained more than 150°, and the contact angle hysteresis increased slightly but remained less than 15°. Next, the nano- and hierarchical structures with CNTs were exposed to water with pressure ranging from 0 to 45 kPa for 20 min. Figure 4a (right side) shows static contact angle and contact angle hysteresis as a function of water pressure. As water pressure hitting the surfaces increased, the static contact angle and contact angle hysteresis decreased and increased slightly, respectively, but a significant change was not found on both nano- and hierarchical structures for superhydrophobicity. It can be interpreted that there was no deformation of CNT structures due to strong bonding with the substrate. As a result, superhydrophobic CNT composite structures showed good stability of wet-

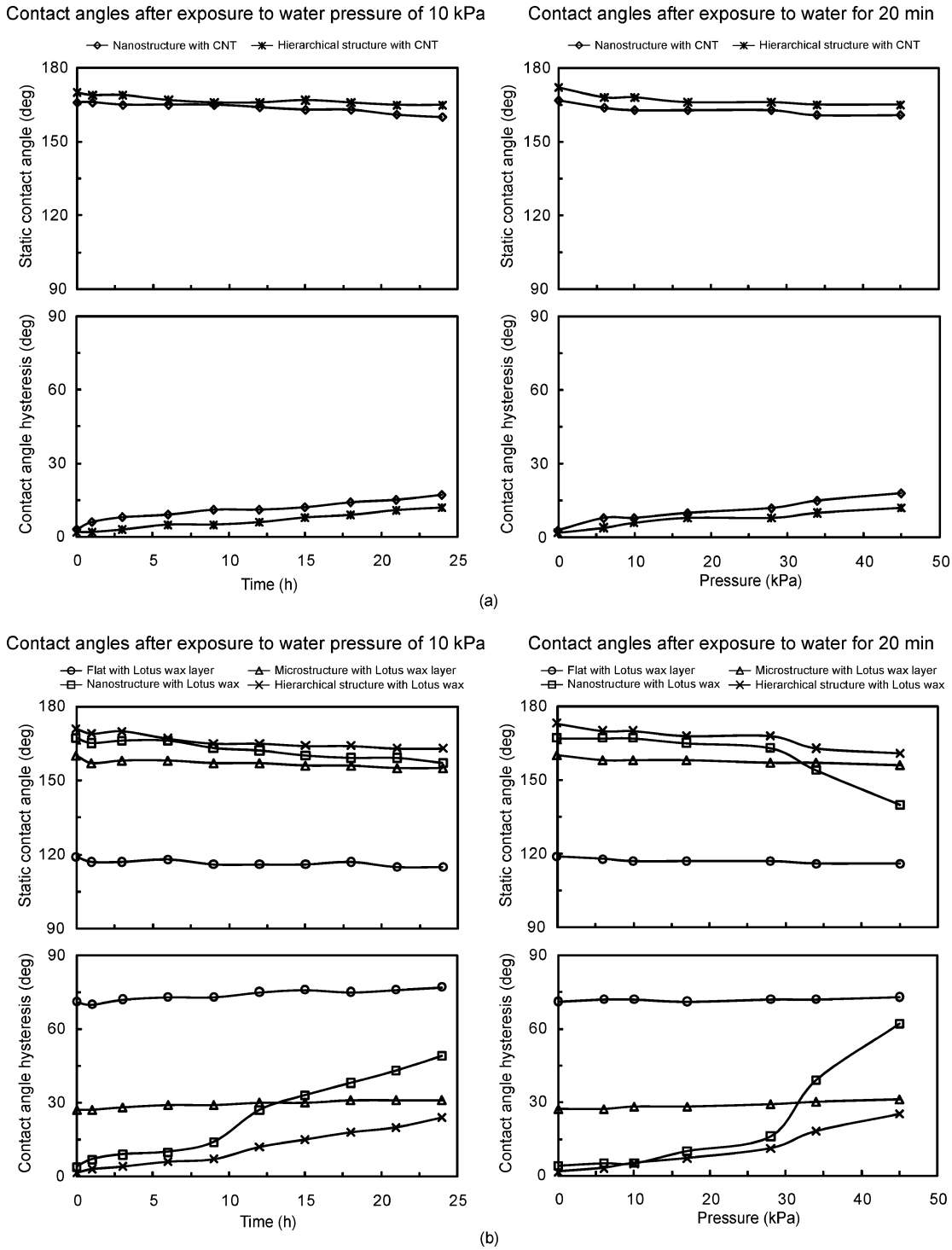

Figure 4. Static contact angle and contact angle hysteresis as a function of exposure time at water pressure of 10 kPa and water pressure of exposure for 20 min for the droplet with a 1 mm radius (5 μL volume) gently deposited on the surfaces with (a) CNTs and (b) lotus wax. The data are reproducible within ±5%.

ting properties not only from long-term exposure to water but also high water pressure.

To compare durability of the created surfaces with CNTs and lotus wax, waterfall/jet tests were also conducted on the flat, nano-, micro-, and hierarchical structures with lotus wax. First, the surfaces with lotus wax were continuously exposed to water pressure of 10 kPa for 24 h. Figure 4b (left side) shows static contact angle and contact angle hysteresis as a function of exposure time. As the exposure time increases up to 24 h, the static contact angle of all samples decreased slightly but remained more than 150°. However, based on contact angle hysteresis data, it was found that after an exposure time of 10 h, the values of nano- and hierarchical structures with lotus wax increased rapidly to 27° and 12° and continued to increase to 49° and 24° at the

exposure time of 24 h, respectively. This indicates that a portion of the wax nanostructured area started to be damaged, resulting in inducing the pinning of the droplet at the damaged area and then increasing contact angle hysteresis. Next, the surfaces with lotus wax were exposed to the water with pressure ranging from 0 to 45 kPa for 20 min. Figure 4b (right side) shows static contact angle and contact angle hysteresis as a function of water pressure of exposure. As the water pressure increased up to 45 kPa, static contact angle and contact angle hysteresis of flat and microstructure with lotus wax layer remained almost constant. However, as the water pressure increased up to 34 kPa, the static contact angle of nano- and hierarchical structures with lotus wax first decreased slightly, and then the contact angle started decreasing sharply. It was also observed that the corresponding large change in contact angle hysteresis was found above 34 kPa. It is usually known that wax structures on the leaves can easily be induced by touching the leaf surface or by mechanical wear during transport of the leaves. As expected, it is observed that the nanostructure with lotus wax can be damaged by water with high pressure, resulting in loss of superhydrophobicity.

Durability of Various Surfaces in AFM and Ball-on-Flat Tribometer Tests. To investigate the durability of the nanostructure fabricated using CNTs, wear tests were conducted by creating 50 × 50 μm^2 wear scars with a 15 μm radius borosilicate ball for 1 cycle at two normal loads of 100 nN and 10 μN using AFM. Figure 5a shows surface height maps before and after wear tests for nanostructures with CNTs. As the normal load of 100 nN was applied on the nanostructure with CNTs, the wear scar induced on the surface after the 100 nN normal load tests was not found or very low, and it was also hard to quantify a wear depth on the nanostructure with CNTs scanned with a borosilicate ball. With an increase of the normal load to 10 μN, it was found that the wear depth on the nanostructure with CNTs was not significantly changed, but the morphology of the CNTs differs slightly from that before wear test. It can be interpreted that the individual CNTs might be expected to slide or bend by the borosilicate ball applied by high normal load of 10 μN during the test process.

For comparison, the durability of the nanostructure fabricated using lotus wax was also investigated by applying two normal loads of 100 nN and 10 μN using AFM. Figure 5b shows surface height maps before and after wear tests for nanostructures with lotus wax. As the normal load of 100 nN was applied on the nanostructure with lotus wax, the change in the morphology of the structured surface was observed, and a small amount of debris was generated compared to the surface before wear test, indicating that the wax nanostructure has weak mechanical strength at even a small load. With increasing the normal load to 10 μN, it was found that the depth of wear mark increased, and the

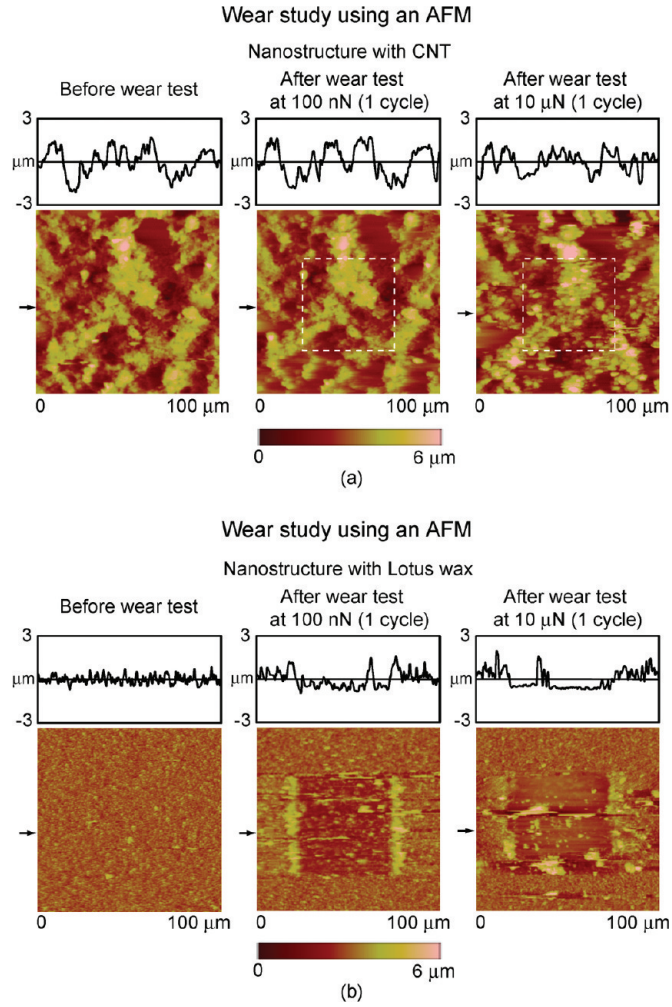

Figure 5. Surface height maps before and after wear tests with a 15 μm radius borosilicate ball at 100 nN and 10 μN for nanostructures with (a) CNTs and (b) lotus wax using an AFM.

nanostructure with lotus wax was fully removed from the substrate. As expected, the nanostructure with lotus wax exhibited the greater amount of wear compared to the nanostructure with CNTs as evidenced by debris build-up around the edge of the wear test region. The damage of the structured surface can cause the sticking of water droplets in the wear region, resulting in low static contact angle and high contact angle hysteresis.

To investigate the durability of structured surfaces at a high load, conventional ball-on-flat tribometer experiments were conducted for the surfaces with CNTs. Figure 6a shows the coefficient of friction as a function of number of cycles for the nano- and hierarchical structures with CNTs. The data are reproducible within ±5% based on three measurements. The coefficients of friction on both nano- and hierarchical structures with CNTs first increased slightly for 20 cycles. Such a trend can be due to the elastic bending or buckling of CNTs by contacting with a sapphire ball during the beginning of the scan, resulting in an increase of the contact area. During the entire experiment, the coefficient of friction

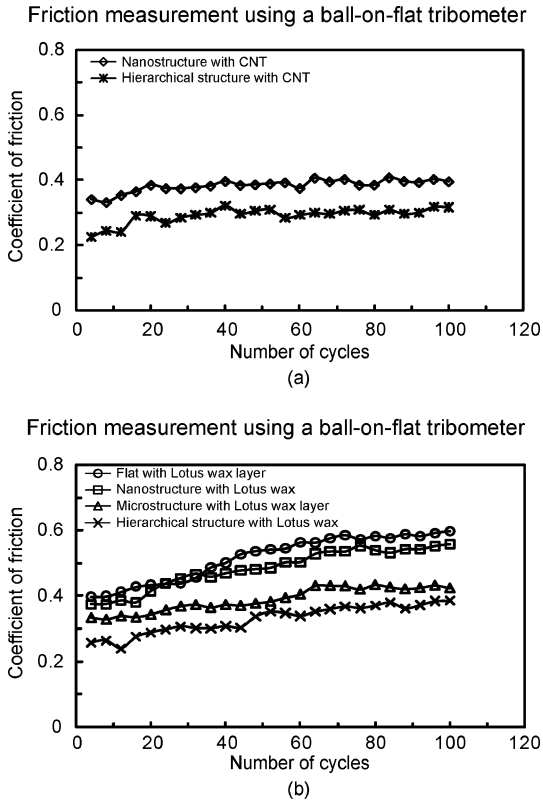

Figure 6. Coefficient of friction as a function of number of cycles using a ball-on-flat tribometer for the surfaces with (a) CNTs and (b) lotus wax at room temperature (22 ± 1 °C) and ambient air (45 ± 5% RH). The data are reproducible within ±5% based on three measurements.

value of the nano- and hierarchical structures with CNTs changed minimally, which indicates that the CNTs was not being worn after 100 cycles. To investigate the change in the morphology of the surfaces after wear test, optical microscope images were obtained before and after wear test as shown in Figure 7a. As expected, it was observed that there is no or low wear on nano- and hierarchical structures after wear tests. No or low wear on the CNT composite structure can possibly be due to the significant increase in the mechanical strength and wear resistance led from the uniform distribution and strong bonding of CNTs on flat epoxy resin and microstructure. The elastic bending or buckling exhibited by CNTs make them exceedingly tough materials and may be absorbing some of the force at contact acting as a compliant spring moderating the impact of the ball on the surface.[40−42]

Contact diameters and contact stresses of CNTs at three loads used in AFM and ball-on-flat tribometer tests were calculated. Table 1 lists the physical properties of various specimens. It is assumed that contacts are single-asperity elastic contacts. For this case, the contact diameter,[38,39]

$$d = 2\left(\frac{3WR}{4E^*}\right)^{1/3} \quad (1)$$

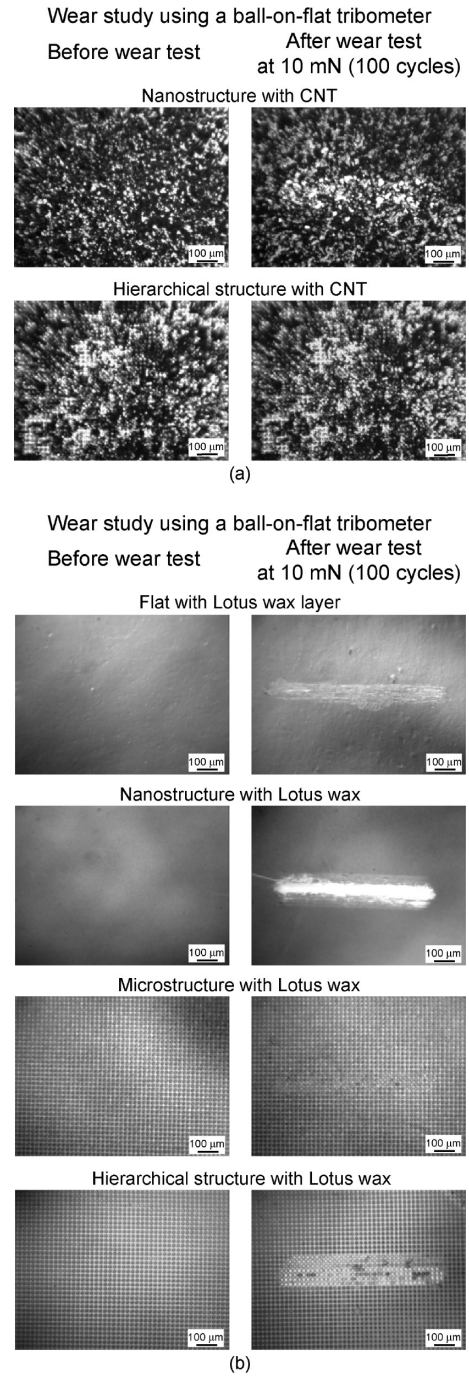

Figure 7. Optical micrographs before and after wear test at 10 mN (100 cycles) using a ball-on-flat tribometer for the surfaces with (a) CNTs and (b) lotus wax.

where W is the total normal load, R is the asperity radius, and E^* is the effective elastic modulus. It should be noted that contact occurs on multiple asperities, and eq 1 gives an approximate value. The calculated contact diameter and contact stress are presented in Table 1. The deformation of CNTs appears to be elastic at the three loads applied by borosilicate ball and sapphire ball.

To compare the durability of the created surfaces with CNTs and lotus wax at a high load, a wear study

TABLE 1. Typical Physical Properties of Various Specimens and Calculated Contact Diameters and Contact Stresses at Three Loads Used in AFM and Ball-on-Flat Tribometer Measurements. It Is Assumed That Contacts Are Single-Asperity Contact

	borosilicate ball with a 15 μm radius	sapphire ball with a 1.5 mm radius	carbon nanotube
elastic modulus (GPa)	70[a]	390[b]	1200[c]
Poisson's ratio	0.2[a]	0.23[b]	0.2[d]
bending strength (GPa)			14.2[c]

	contact diameter (μm)			mean contact pressure (GPa)		
	borosilicate ball at 100 nN	borosilicate ball at 10 μN	sapphire ball at 10 mN	borosilicate ball at 100 nN	borosilicate ball at 10 μN	sapphire ball at 10 mN
carbon nanotube	0.05	0.24	6.62	0.076	0.33	0.44

[a]Callister.[43] [b]Bhushan and Gupta.[44] [c]Wong *et al.*[45] [d]Zhang *et al.*[46]

was conducted on the surfaces with lotus wax using a conventional ball-on-flat tribometer. As shown in Figure 6b, the coefficient of friction value of the surfaces with lotus wax exhibited a gradual increase when the sliding cycle increases up to about 70 cycles, and then remains constant. This indicates that the wax nanostructure and flat wax layer could be undergoing some wear due to weak bonding between them and the substrates. The change in the morphology of the surfaces with lotus wax was observed in optical microscope images as shown in Figure 7b. As shown in the AFM study at low loads (Figure 5b), it is clearly observed that the flat wax layer and wax nanostructure on flat and microstructure were fully removed from the surfaces. As a result, superhydrophobic CNT composite structures showed better mechanical durability than the structured surfaces with lotus wax to best withstand real world applications.

CONCLUSIONS

To create mechanically durable structured surfaces with superhydrophobicity, self-cleaning, and low-drag, CNT composite structures were produced by replication of a micropatterned silicon surface using an epoxy resin and by deposition of the CNT composite using a spray method. The hierarchical structure created with CNTs showed a high static contact angle of 170° and a low contact angle hysteresis of 2°. As a benchmark, the structures created using lotus wax were used to compare the durability of CNT composite structures. To investigate durability of the fabricated surfaces, waterfall/jet tests were conducted to determine the loss of superhydrophobicity, and wear and friction studies were also performed using AFM and ball-on-flat tribometer. It was found that superhydrophobic CNT composite structures showed good stability of wetting properties not only from long-term exposure to water but also high water pressure. In contrast, it was observed that the nanostructure with lotus wax can be damaged by water with high pressure, resulting in the loss of superhydrophobicity. From wear and friction studies, it was found that the nanostructure with lotus wax can be easily damaged at even a small load. However, the CNT composite structure showed high mechanical strength and wear resistance led from the uniform distribution and strong bonding of CNTs on flat epoxy resin and microstructure to best withstand real world applications.

EXPERIMENTAL DETAILS

Samples. Microstructures were fabricated using a microstructured Si surface with pillars of 14 μm diameter and 30 μm height with 23 μm pitch by soft lithography.[4,17] The replication is a two-step molding process, in which a negative replica of a template is generated using a polyvinylsiloxane dental wax and a positive replica is made with a liquid epoxy resin (contact angle about 80°).

To create nano- and hierarchical structures with a high mechanical strength, multiwalled CNTs were fabricated using catalyst-assisted chemical vapor deposition (CCVD) (Sun Nanotech Co Ltd., China). Iron catalyst was used to initiate growth of nanotubes using natural gas as the carbon source and Ar/H_2 as buffer gas at 750 °C. The contact angle of individual carbon nanotubes has been reported as 60° and higher. The multiwalled CNT composites were deposited on flat epoxy resin and microstructure using a spray method as shown in Figure 8. The first step of the spray method was to disperse the CNTs into a solvent in order to maintain a uniform distribution. Acetone was used as a solvent because it does not affect surface modification and is easily vaporized in ambient conditions. The dispersion process consists of the sonification of 200 mg of CNTs in 100 mL of acetone for 4 min using a Branson digital sonifier with a frequency of 20 kHz at amplitude of 80%. During this process, the mixture was exposed to ultrasonic pressure waves in a sonifier in order to disperse the CNTs into smaller aggregates. To provide strong bonding between CNTs and the substrate, 200 mg of EPON epoxy resin 1002F was added to the mixture of CNTs and acetone, and then the mixture was sonificated for 4 more minutes. Next, the sonified mixture was poured into a spray gun and sprayed onto the specimen surfaces. The conditions for uniform deposition of the CNTs on the surfaces were optimized by adjusting the concentration of CNTs in the solvent. After spraying the CNTs on the surfaces, the CNT composite structures were then annealed at 120 °C for 3 h in order to improve the mechanical properties. This temperature, above the melting point (80−88 °C) and below the burning point (180 °C) of EPON epoxy resin 1002F, was selected to increase strong bonding be-

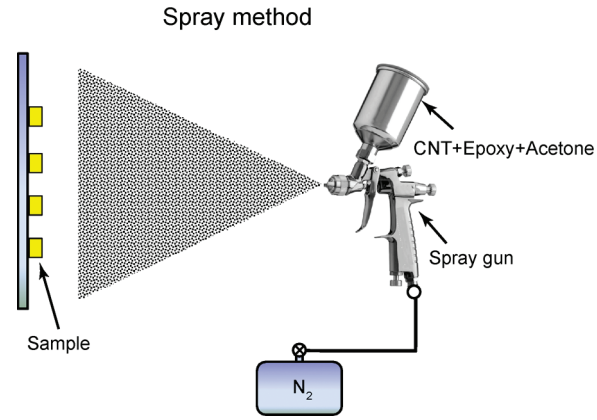

Figure 8. Schematic of spray method to deposit a mixture of CNTs, epoxy, and acetone on surfaces.

tween CNTs and substrates. At this temperature, the epoxy which initially covered the CNTs was melted and moved to the interface between the CNTs and substrates, resulting in exposed CNTs which lead to high contact angle.

Lotus leaves have been the inspiration for the development of superhydrophobic and self-cleaning products. Therefore, as a benchmark for mechanical durability studies, nano- and hierarchical structures were created by the self-assembly of lotus wax with the amounts of 0.8 $\mu g/mm^2$ deposited on flat epoxy resin and microstructure by thermal evaporation.[4,17] The specimens with lotus wax were exposed to ethanol vapor for 3 days at 50 °C, and then left in the oven at 50 °C for 7 days in total. Flat epoxy resin and a microstructure were covered with a flat lotus wax layer. Flat wax layers were made by melting the deposited wax (3 min at 120 °C) and subsequent rapid cooling of the specimen to 5 °C. Then the specimens were stored for 7 days at 21 °C in a desiccator. The fast cooling of the wax prevents the formation of nanostructure roughness.

Waterfall/Jet Tests. To investigate durability of the created surfaces in long-term exposure to water and different kinetic energies of water, a setup was constructed to provide a waterfall/jet flow as shown in Figure 9. The water from the laboratory faucet flowed through a pipe. Specimens were fixed on the stage by using a double-sided adhesive tape. Specimens are placed 2 mm below the four holes in the pipe. To minimize flow interruption on the specimens, the runoff plate was tilted to 45°. Waterfall/jet experiments are composed of two different setups. First, water pressure was fixed at 10 kPa, and then specimens were exposed for 24 h. Next, to apply different kinetic energies of the water, the water pressure was controlled between 0 and 45 kPa. The exposure time applied to the specimens was 20 min for each experiment. During the tests, the change of static contact angle was measured using droplets of about 5 μL in volume (with radius of a spherical droplet about 1 mm) gently deposited on the substrate using a microsyringe. For contact angle hysteresis, the advancing and receding contact angles were measured at the front and back of the droplet moving along the tilted surface, respectively. The image of the droplet is obtained by a digital camcorder (Sony, DCRSR100, Tokyo, Japan) with a 10× optical and 120× digital zoom. Images obtained were analyzed using Imagetool software (University of Texas Health Science Center) for the contact angle.

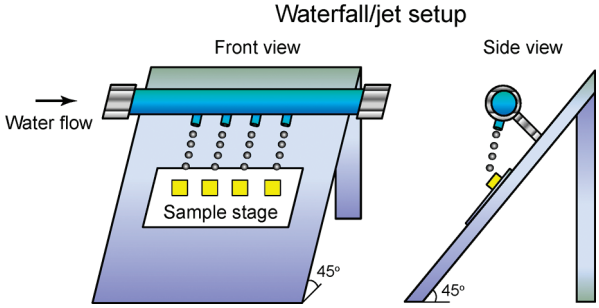

Figure 9. Schematics of waterfall/jet setup shown in front and side views.

Wear and Friction Tests. To investigate the durability of structured surfaces, wear tests on the surfaces with CNT and lotus wax were performed using a commercial AFM (D3100, Nanoscope IIIa controller, Digital Instruments, Santa Barbara, CA). With the AFM in contact mode, the surfaces with CNT and lotus wax were worn using a 15 μm radius borosilicate ball that was mounted on a triangular Si_3N_4 cantilever with a nominal spring constant of 0.58 N m^{-1}. Wear scars with dimensions of 50 × 50 μm^2 were created and scanned for one cycle at two different loads of 100 nN and 10 μN. To analyze the changes in the morphology of structured surfaces before and after wear tests, surface height maps were obtained in dimensions of 100 × 100 μm^2 using a square pyramidal Si(100) tip with a native oxide layer which has a nominal radius of 20 nm on a rectangular Si(100) cantilever with a spring constant of 3 N m^{-1} and at a natural frequency of 76 kHz in tapping mode.

To investigate durability at a high load, macroscale wear and friction tests on the surfaces with CNTs and lotus wax were conducted on the basis of an established procedure of using a ball-on-flat tribometer under reciprocating motion.[37−39] A sapphire ball with a diameter of 3 mm and surface finish of about 2 nm rms was fixed on a stationary holder. A normal load of 10 mN was applied, and the frictional forces were measured with semiconductor strain gauges, which were then digitized and collected on a computer. Typical test conditions were as follows: stroke length = 800 μm, average linear speed = 1 mm/s, temperature = 22 ± 1 °C, and relative humidity = 45 ± 5%. Wear was characterized by imaging the resulting scar with an optical microscope with a CCD camera (Nikon, Optihot-2) before and after wear tests. The number of cycles to failure was determined by identifying the point where a sudden change in the friction force is observed.

REFERENCES AND NOTES

1. Bhushan, B. *Springer Handbook of Nanotechnology,* 2nd ed; Springer: Heidelberg, Germany, 2007.
2. Bhushan, B.; Jung, Y. C. Wetting, Adhesion and Friction of Superhydrophobic and Hydrophilic Leaves and Fabricated Micro/Nanopatterned Surfaces. *J. Phys.: Condens. Matter* **2008**, *20*, 225010.
3. Nosonovsky, M.; Bhushan, B. *Multiscale Dissipative Mechanisms and Hierarchical Surfaces: Friction, Superhydrophobicity, and Biomimetics*; Springer-Verlag: Heidelberg, Germany, 2008.
4. Bhushan, B.; Jung, Y. C.; Koch, K. Micro-, Nano- and Hierarchical Structures for Superhydrophobicity, Self-Cleaning and Low Adhesion. *Phil. Trans. R. Soc., A* **2009**, *367*, 1631–1672.
5. Barthlott, W.; Neinhuis, C. Purity of the Sacred Lotus, or Escape from Contamination in Biological Surfaces. *Planta* **1997**, *202*, 1–8.
6. Koch, K.; Bhushan, B.; Barthlott, W. Diversity of Structure, Morphology, and Wetting of Plant Surfaces (invited). *Soft Matter* **2008**, *4*, 1943–1963.
7. Koch, K.; Bhushan, B.; Barthlott, W. Multifunctional Surface Structures of Plants: An Inspiration for Biomimetics (invited). *Prog. Mater. Sci.* **2009**, *54*, 137–178.
8. Patankar, N. A. Mimicking the Lotus Effect: Influence of Double Roughness Structures and Slender Pillars. *Langmuir* **2004**, *20*, 8209–8213.
9. Li, W.; Amirfazli, A. Hierarchical Structures for Natural Superhydrophobic Surfaces. *Soft Matter* **2008**, *4*, 462–466.
10. Shirtcliffe, N. J.; McHale, G.; Newton, M. I.; Chabrol, G.; Perry, C. C. Dual-Scale Roughness Produces Unusually Water-Repellent Surfaces. *Adv. Mater.* **2004**, *16*, 1929–1932.
11. Ming, W.; Wu, D.; van Benthem, R.; de With, G. Superhydrophobic Films from Raspberry-like Particles. *Nano Lett.* **2005**, *5*, 2298–2301.
12. Sun, M.; Luo, C.; Xu, L.; Ji, H.; Ouyang, Q.; Yu, D.; Chen, Y. Artificial Lotus Leaf by Nanocasting. *Langmuir* **2005**, *21*, 8978–8981.

13. Chong, M. A. S.; Zheng, Y. B.; Gao, H.; Tan, L. K. Combinational Template-Assisted Fabrication of Hierarchically Ordered Nanowire Arrays on Substrates for Device Applications. *Appl. Phys. Lett.* **2006**, *89*, 233104.
14. del Campo, A.; Greiner, C. SU-8: A Photoresist for High-Aspect-Ratio and 3D Submicron Lithography. *J. Micromech. Microeng.* **2007**, *17*, R81–R95.
15. Cortese, B.; Amone, S. D.; Manca, M.; Viola, I.; Cingolani, R.; Gigli, G. Superhydrophobicity Due to the Hierarchical Scale Roughness of PDMS Surfaces. *Langmuir* **2008**, *24*, 2712–2718.
16. Zhao, Y.; Li, M.; Lu, Q.; Shi, Z. Superhydrophobic Polyimide Films with a Hierarchical Topography: Combined Replica Molding and Layer-by-Layer Assembly. *Langmuir* **2008**, *24*, 12651–12657.
17. Koch, K.; Bhushan, B.; Jung, Y. C.; Barthlott, W. Fabrication of Artificial Lotus Leaves and Significance of Hierarchical Structure for Superhydrophobicity and Low Adhesion. *Soft Matter* **2009**, *5*, 1386–1393.
18. Kuan, C. Y.; Hon, M. H.; Chou, J. M.; Leu, I. C. Wetting Characteristics on Micro/Nanostructured Zinc Oxide Coatings. *J. Electrochem. Soc.* **2009**, *156*, J32–J36.
19. Lau, K. K. S.; Bico, J.; Teo, K. B. K.; Chhowalla, M.; Amaratunga, G. A. J.; Milne, W. I.; McKinley, G. H.; Gleason, K. K. Superhydrophobic Carbon Nanotube Forests. *Nano Lett.* **2003**, *3*, 1701–1705.
20. Huang, L.; Lau, S. P.; Yang, H. Y.; Leong, E. S. P.; Yu, S. F.; Prawer, S. Stable Superhydrophobic Surface *via* Carbon Nanotube Coated with ZnO Thin Film. *J. Phys. Chem. B* **2005**, *109*, 7746–7748.
21. Yurdumakan, B.; Raravikar, N. R.; Ajayan, P. M.; Dhinojwala, A. Synthetic Gecko Foot-Hairs from Multiwalled Carbon Nanotubes. *Chem. Commun.* **2005**, *2005*, 3799–3801.
22. Zhu, L.; Xiu, Y.; Xu, J.; Tamirisa, P. A.; Hess, D. W.; Wong, C.-P. Superhydrophobicity on two-tier rough surfaces fabricated by controlled growth of aligned carbon nanotube arrays coated with fluorocarbon. *Langmuir* **2005**, *21*, 11208–11212.
23. Hong, Y. C.; Uhm, H. S. Superhydrophobicity of a Material Made from Multiwalled Carbon Nanotubues. *Appl. Phys. Lett.* **2006**, *88*, 244101.
24. Chen, C.-H.; Qingjun, C.; Tsai, C.; Chen, C.-L. Dropwise Condensation on Superhydrophobic Surfaces with Two-Tier Roughness. *Appl. Phys. Lett.* **2007**, *90*, 173108.
25. Schadler, L. S.; Giannaris, S. C.; Ajayan, P. M. Load Transfer in Carbon Nanotube Epoxy Composites. *Appl. Phys. Lett.* **1998**, *73*, 3842–3844.
26. Qian, D.; Dickey, E. C.; Andrews, R.; Ranell, T. Load Transfer and Deformation Mechanism in Carbon Nanotube−Polystyrene Composites. *Appl. Phys. Lett.* **2000**, *76*, 2868–2870.
27. Chen, W. X.; Tu, J. P.; Wang, L. Y.; Gan, H. Y.; Xu, Z. D.; Zhang, X. B. Tribological Application of Carbon Nanotubes in a Metal-Based Composite Coating and Composites. *Carbon* **2003**, *41*, 215–222.
28. Shi, D.; Lian, J.; He, P.; Wang, L. M.; Xiao, F.; Yang, L.; Schulz, M. J.; Mast, D. B. Plasma Coating of Carbon Nanofibers for Anhanced Dispersion and Interfacial Bonding in Polymer Composites. *Appl. Phys. Lett.* **2003**, *83*, 5301–5303.
29. Yang, Z.; Dong, B.; Huang, Y.; Liu, L.; Yan, F.-Y.; Li, H.-L. A Study on Carbon Nanotubes Reinforces Poly(methyl methacrylate) Nanocomposites. *Mater. Lett.* **2005**, *59*, 2128–2132.
30. Lee, H.; Mall, S.; He, P.; Shi, D.; Narasimhadevara, S.; Yeo-Heung, Y.; Shanov, V.; Shulz, M. J. Characterization of Carbon Nanotube/Nanofiber-Reinforced Polymer Composites Using an Instrumented Indentation Technique. *Composites: Part B* **2007**, *38*, 58–65.
31. Madou, M. *Fundamentals of Microfabrication*; CRC Press: Boca Raton, FL, 1997.
32. Varadan, V. K.; Jiang, X.; Varadan, V. V. *Microstereolithography and Other Fabrication Techniques for 3D MEMS*; Wiley: New York, 2001.
33. Jeong, H. J.; Choi, H. K.; Kim, G. Y.; Song, Y. I.; Tong, Y.; Lim, S. C.; Lee, Y. H. Fabrication of Efficient Field Emitters with Thin Multiwalled Carbon Nanotubes Using Spray Method. *Carbon* **2006**, *44*, 2689–2693.
34. Yang, J.; Zhang, Z.; Men, X.; Xu, X. Fabrication of Stable, Transparent and Superhydrophobic Nanocomposite Films with Polystyrene Functionalized Carbon Nanotubes. *Appl. Surf. Sci.* **2009**, *255*, 9244–9247.
35. Bhushan, B. *Handbook of Micro/Nanotribology*, 2nd ed.; CRC Press: Boca Raton, FL, 1999.
36. Bhushan, B. *Nanotribology and Nanomechanics - An Introduction*; 2nd ed., Springer-Verlag: Heidelberg, Germany, 2008.
37. Bhushan, B.; Gupta, B. K.; Azarian, M. H. Nanoindentation, microscratch, friction and wear studies of coatings for contact recording applications. *Wear* **1995**, *181−183*, 743–758.
38. Bhushan, B. *Principles and Applications of Tribology*; Wiley: New York, 1999.
39. Bhushan, B. *Introduction to Tribology*; Wiley: New York, 2002.
40. Dresselhaus, M. S.; Dresselhaus, G.; Avouris, Ph. *Carbon Nanotubes: Synthesis, Structure, Properties, and Applications*; Springer: Heidelberg, Germany, 2000.
41. Meyyappan, M. *Carbon Nanotubes - Science and Applications*; CRC Press: Boca Raton, FL, 2005.
42. Chen, X. H.; Chen, C. S.; Xiao, H. N.; Liu, H. B.; Zhou, L. P.; Li, S. L.; Zhang, G. Dry friction and wear characteristics of nickel/carbon nanotube electroless composite deposits. *Tribol Int* **2006**, *39*, 22–28.
43. Callister, W. D. *Materials Science and Engineering - An Introduction*; 5th ed., John Wiley and Sons: New York, 2000.
44. Bhushan, B.; Gupta, B. K. *Handbook of Tribology: Materials, Coatings, and Surface Treatments*; McGraw-Hill: New York, 1991.
45. Wong, E. W.; Sheehan, P. E.; Lieber, C. M. Nanobeam Mechanics: Elasticity, Strength, and Toughness of Nanorods and Nanotubes. *Science* **1997**, *277*, 1971–1975.
46. Zhang, Y. Y.; Wang, C. M.; Tan, V. B. C. Examining the Effects of Wall Numbers on Buckling Behavior and Mechanical Properties of Multiwalled Carbon Nanotubes *via* Molecular Dynamics Simulations. *J. Appl. Phys.* **2008**, *103*, 053505.